

1 **TO REFEREE #1**

2 Thank you very much for all your suggestions and comments. Next, we respond all your
3 suggestions in order.

4 1. About Table 2:

5 We have modified the table 2 eliminating redundant information.

6 2. About HSL filtering method:

7 We establish a relationship between the color of the satellite image and the color
8 of the pasture contained in this image. Saturations lower than 0.15 are
9 inconsistent with dry (low NDVI values) or healthy (high NDVI values) pasture and
10 highly correlated with pasture covered by clouds or snow. Thus, this method uses a
11 color criterion to eliminate wrong NDVI values.

12 3. About the number of observations of every RV (interval):

13 The theoretical number of observations for every RV is: 6 pixels x 16 year = 96
14 observations. We have lost some observations after applying the HSL filtering
15 method. We have modified the word "sample" by "observations" to avoid
16 misunderstanding.

17 4. About the level of significance:

18 You are right, we missed this important value. We have included it in the results.
19 Now you can read: "The level of significance (α) was fixed to 5% for all the
20 candidates".

21 5. About Figure 5:

22 You are right, Fig. 5 shows the percentage of adjusted intervals (RVs) for each
23 candidate distribution. We have added more information in the figure caption.
24 Now you can read: "Figure 5. Percentage of fitted intervals (Y axis) for each PDF
25 candidate (Normal, Gamma, Beta and GEV distributions) in function of the number
26 of classes (X axis)."

27 6. Is there any relationship between the season and the number of intervals that fit
28 correctly for each type of distribution?

29 When we filter the data by season we find that GEV distributions explain better
30 some intervals of spring and autumn since their observed distributions are very
31 asymmetric. On the other hand, we do not find an important difference in winter,
32 since its observed distributions are mainly symmetric in these intervals.

33 7. What is the proportion from which you consider that percentage is satisfactory?.

34 In this study we do not want to affirm that GEV is the best distribution because fits
35 better than the others. Our objective is to notice that could exist others
36 alternatives to Normal distributions. With respect the selected distributions in this

37 study we can affirm that 40% (GEV distribution) is highly enough to at least not
38 consider the Normal distribution.

39 8. "... you have not statistically evaluated the differences between GEV distribution
40 and other tri-parametric distributions (Generalized Pareto, Normal Log, ...":

41 The objective of this study is not to find the best fit for the observed NDVI
42 distribution, but to highlight that Normal distribution could not be the best fit. To
43 avoid this imprecision we recommend the use of quantiles to calculate damage
44 pasture thresholds.

45 9. Differences between interval 35 and 36:

46 These two intervals belong to autumn and this season is characterized by its high
47 variability. If you observe the NDVI distributions in the appendix A for these two
48 intervals, you can notice how the distribution is changing from summer (with a
49 strong peak) to autumn (with an incipient tail).

50 10. In figure 3 it is necessary to define the axis of abscissa:

51 Now you can see this information in the figure.

52 11. Clarify in the text that intervals go consecutively from 8 to 8 days, indicating the
53 start intervals of each season:

54 We have modified the first paragraph of section 3.2. Now you can read: "NDVI
55 values were obtained consecutively every 8 days from MODIS product starting at
56 1st of January of every year, in such a way that 46 NDVI observations were
57 considered for each year. Therefore, 46 Random Variables (RV) were defined when
58 taking into account all the years of this study.

59 In Table 2, every RV (named as "Interval") can be seen together with the number
60 of available NDVI observations. Each RV collects the observations coming from the
61 six selected pixels. The start intervals of each season are: interval 45 for winter,
62 interval 11 for spring, interval 23 for summer and interval 34 for autumn."

63

64

Statistical Analysis for Satellite Index-Based Insurance to define Damaged Pasture Thresholds

Juan José Martín-Sotoca^{1*}, Antonio Saa-Requejo^{2,3}, Rubén Moratíel^{2,3}, Nicolas Dalezios⁴, Ioannis Faraslis⁵, and Ana María Tarquis^{2,6}

jmartinsotoca@gmail.com, antonio.saa@upm.es, ruben.moratíel@upm.es, dalezios.n.r@gmail.com, faraslisgiannis@yahoo.gr, anamaria.tarquis@upm.es

¹ Data Science Laboratory. European University, Madrid, Spain.

² CEIGRAM, Research Centre for the Management of Agricultural and Environmental Risks, Madrid, Spain.

³ Dpto. Producción Agraria. Universidad Politécnica de Madrid, Spain.

⁴ Department of Civil Engineering. University of Thessaly, Volos, Greece.

⁵ Department of Planning and Regional Development. University of Thessaly, Volos, Greece.

⁶ Grupo de Sistemas Complejos. Universidad Politécnica de Madrid, Spain.

* Correspondence to: jmartinsotoca@gmail.com

Abstract: Vegetation indices based on satellite images, such as Normalized Difference Vegetation Index (NDVI), have been used in countries like USA, Canada and Spain for damaged pasture and forage insurance for the last years. This type of agricultural insurance is called “satellite index-based insurance” (SIBI). In SIBI, the occurrence of damage is defined through NDVI thresholds mainly based on statistics derived from Normal distributions. In this work a pasture area at the north of Community of Madrid (Spain) has been delimited by means of Moderate Resolution Imaging Spectroradiometer (MODIS) images. A statistical analysis of NDVI histograms was applied to seek for the best statistical distribution using maximum likelihood method. The results show that the Normal distribution is not the optimal representation and the General Extreme Value (GEV) distribution presents a better fit through the year. A comparison between Normal and GEV are showed respect to the probability under a NDVI threshold value along the year. This suggests that a priori distribution should not be selected and a percentile methodology should be used to define a NDVI damage threshold rather than the average and standard deviation, typically of Normal distributions.

Keywords: NDVI, pasture insurance, GEV distribution, MODIS.

Highlights

- General Extreme Value (GEV) distribution provides the best fit to the NDVI historical observations.
- Difference between Normal and GEV distributions are higher during spring and autumn, transition periods in the precipitation regimen.
- NDVI damage threshold shows evident differences using Normal and GEV distributions covering both the same probability (24.20%).

- **NDVI damage threshold values based on percentiles calculation is proposed as an improvement in the index based insurance in damaged pasture.**

1. Introduction

Agricultural insurance addresses the reduction of the risk associated with crop production and animal husbandry. The concept of index-based insurance (IBI) attempts to achieve settlements based on the value taken by an objective index rather than on a case-by-case assessment of crop or livestock losses (Gommes and Kayitakier, 2013). Indeed, the goal of IBI policy remains to develop an affordable tool to all producers, including smallholders. Specifically, IBI can constitute a safety net against weather-related risks for all members of the farming community, thereby increasing food security and reducing the vulnerability of rural populations to weather extremes. Moreover, IBI can be associated with credits for insured smallholders, due to the fact that the risk of non-repayment for lenders is reduced, which encourages the use of agricultural inputs and equipment, leading to increased and more stable crop production. Over the past decade, the importance of weather index-based insurances (WIBI) for agriculture has been increasing, mainly in developing countries (Gommes and Kayitakier, 2013). This interest can be explained by the potential that IBI constitutes a risk management instrument for small farmers. Indeed, it can be considered within the context of renewed attention to agricultural development as one of the milestones of poverty reduction and increased food security, as well as the accompanying efforts from various stakeholders to develop agricultural risk management instruments, including agricultural insurance products.

Farmers need to protect their land and crops specifically from drought in arid and semi-arid countries, since their production may directly depend mainly on the impacts of this particular natural hazard. Insurance for drought-damaged lands and crops is currently the main instrument and tool that farmers can resort in order to deal with agricultural production losses due to drought. Many of these insurances are using satellite vegetation indices (Rao, 2010), thus they are also called “satellite index-based insurances” (SIBI). SIBI have some advantages over WIBI, such as cost-effective information and acceptable spatial and temporal resolution. They do not, however, resolve the issue of basis risk, i.e. potential unfairness to insurance takers (Leblois, 2012). Moreover, the very nature of an index-based product creates the chance that an insured party may not be paid when they suffer loss. For this reason, in some countries (Spain) they have named this SIBI as “damaged in pasture” to cover not only drought even this one is the main cause.

139 It is highly recognized that shortage of water has many implications to agriculture,
140 society, economy and ecosystems. Specifically, its impact on water supply, crop
141 production and rearing of livestock is substantial in agriculture. Knowing the likelihood of
142 drought is essential for impact prevention (Dalezios, 2013). Drought severity assessment
143 can be approached in different ways: through conventional indices based on
144 meteorological data, such as temperature, rainfall, moisture, etc. (Niemeyer, 2008), as
145 well as through remote sensing indices based on images usually taken by artificial
146 satellites (Lovejoy et al., 2008) or drones. In the second group they are found Satellite
147 Vegetation Indices (SVI), which can quantify “green vegetation”, and soil moisture through
148 Soil Water Index (Gouveia et al., 2009) combining different spectral reflectances. Thus,
149 they are one of the main ways to quantitatively assess drought severity.

150

151 At the present time, several satellites (NOAA, TERRA, DEIMOS, etc.) can provide this
152 spectral information with different spatial resolution. Some series with a high temporal
153 frequency are freely available, those from NOAA satellites and Terra. The most widely
154 known SVI is the Normalized Difference Vegetation Index (NDVI). It follows the principle
155 that healthy vegetation mainly reflects the near-infrared frequency band. There are
156 several other important SVI, such as Soil Adjusted Vegetation Index (SAVI) and Enhanced
157 Vegetation Index (EVI) that incorporate soil effects and atmospheric impacts, respectively.
158 An important point of this class of insurance is “when damage occurs”. To measure this, a
159 SVI threshold value is defined mainly based on statistics that apply to Normal distributed
160 variables: average and standard deviation. When current SVI values are below this
161 threshold value for a period of time, insurance recognizes that a damage is occurring,
162 most of the times drought, and then it begins to pay compensations to farmers.

163

164 WIBI aims to protect farmers against weather-based disasters such as droughts, frosts
165 and floods. A WIBI policy links possible insurance payouts with the weather requirements
166 of the crop being insured: the insurer pays an indemnity whenever the realized value of
167 the weather index meets a specified threshold. Whereas payouts in traditional insurance
168 programs are related to actual crop damages, a farmer insured under a WIBI contract may
169 receive a payout. A current difficulty to the wide implementation of WIBI is the weakness
170 of indices. Indeed, there is certainly a need for more efficient indices based on the
171 additional experience gained from the implementation of WIBI products in the developing
172 world. Current trends in index technology are exciting and they actuate high expectations,
173 especially the development of yield indices and the use of remote sensing inputs. Risk
174 protection and insurance illiteracy constitute another difficulty, which has to be addressed
175 by training and awareness-raising at all levels, from farmers to farmers’ associations,
176 micro-insurance partners, as well as senior decision-makers in insurance, banking, and

177 politics (Bailey, 2013). It is essential that all stakeholders (especially the insured) perfectly
178 understand the principles of IBI, as otherwise the insurer, even the whole concept of
179 insurance, is at risk of reputation loss for years or decades.

180

181 There is currently a lack of technical capacity in the insurance sectors of most
182 developing countries, which is a constraint to the scaling up and further development of
183 WIBI (Gommes and Kayitakire, 2012). Specifically, although it is possible to design an index
184 product and assist in roll-out, marketing, and sales, such assistance is not possible on a
185 wide scale, simply because there is lack of qualified expertise. Indeed, it usually requires
186 mathematical modeling, data manipulation, and expertise in crop simulation to design an
187 index. Nevertheless, it is possible to structure insurance with multiple indices, but this
188 increases the complexity of the product and makes it difficult for farmers to comprehend
189 it. ‘Basis risk’ is also a particular problem for index products, which is frequently caused by
190 the fact that measurements of a particular variable, such as rain, may differ at the
191 insurer’s measurement site and in the farmer’s field. This also creates problems for
192 insurance providers. Indeed, part of the reason the scaling up of index products has failed
193 is that both insurers and farmers suffer from this basis risk.

194

195 Currently, to mitigate impacts of climate-related reduced productivity of French
196 grasslands, several studies have been developed to design new insurance scheme bases
197 indemnity payouts to farmers on a forage production index (FPI) (Rumiguié et al., 2015;
198 2017). Two examples of SIBIs are presented in two different countries: USA and Spain. In
199 particular, in USA there are several insurance programs for pasture, rangeland and forage,
200 which use various indexing systems (rainfall and vegetation indices), and are promoted by
201 Unites States Department of Agriculture (USDA) (Maples et al., 2016; USDA, 2018). NDVI is
202 the index chosen in the vegetation index program and it is obtained from AVHRR
203 (Advanced Very High Resolution Radiometer) sensor onboard NOAA satellites. Average,
204 maximum and minimum NDVI values are obtained from a historical series with the aim of
205 calculating a trigger value. Insurer decides the quantity of compensation comparing this
206 trigger with current value. On the other hand, in Spain there exists the “Insurance for
207 Damaged Pasture” from “Spanish System of Agricultural Insurance” (BOE, 2013). This
208 insurance defines damage event through NDVI values obtained from MODIS sensor
209 onboard TERRA satellite of NASA. In this insurance, NDVI threshold values ($NDVI_{th}$) are
210 calculated subtracting several times ($k = 0.7$ or $k = 1.5$) standard deviation to average
211 within a homogeneous area:

212

213

214

$$NDVI_{th} = \mu - k \cdot \sigma \quad (1)$$

215 where μ, σ are average and standard deviation of NDVI respectively. Average and standard
216 deviation come of supposing Normal distributions in the historical data (Goward et al.,
217 1985; Hobbs, 1995; Fuller, 1998; Al-Bakri and Taylor, 2003; Turvey et al., 2012; De Leeuw
218 et al. 2014).

219

220 The aim of this paper is to find a more realistic statistical NDVI distribution without
221 the “a priori” assumption that variables follow a Normal distribution, typically for current
222 SIBI methodology. In order to achieve this, the Maximum Likelihood Method (MLM) is
223 fitted to a historical series of NDVI values in a pasture land area in Spain (Community of
224 Madrid). Different types of asymmetrical distributions are examined with the aim to find a
225 better fit than Normal. To eliminate some noise in the historical series, an original method
226 is applied consisting of using Hue-Saturation-Lightness (HSL) color model. Finally, Chi-
227 square test (χ^2 test) has been used to check the goodness of fit for all considered
228 distributions.

229

230

231 **2. Materials and Methods**

232 **2.1 Vegetation Index**

233 The differences of the reflectance of green vegetation in parts of the electromagnetic
234 radiation spectrum, namely, visible and near infrared, provide an innovative method for
235 monitoring surface vegetation from space. Specifically, the spectral behavior of vegetation
236 cover in the visible (0.4-0.7mm) and near infrared (0.74-1.1mm, 1.3-2.5mm) offers the
237 possibility to monitor from space the changes in the different stages of cultivated and
238 uncultivated plants taking also into account the corresponding behavior of the
239 surrounding microenvironment (Ortega-Farias et al., 2016). Indeed, from the visible part
240 of the electromagnetic radiation spectrum it is possible to draw conclusions about the
241 rate photosynthesis, whereas from near infrared inferences are extracted about the
242 chlorophyll density and the amount of canopy in the plant mass, as well as the water
243 content in the leaves, which is also linked directly to the rate of transpiration with impacts
244 to physiological process of photosynthesis. Usually, data from NOAA/AVHRR series of
245 polar orbit meteorological satellites are used with low spatial resolution (1.1 km^2) and
246 recurrence interval at least twice daily from the same location. Several algorithms
247 combining channels of red (RED), near infrared (NIR) and green (GREEN) have been
248 proposed, which provide indices sensitive to green vegetation.

249

250 NDVI uses two frequency bands: red band (660 nm) and near-infrared band (860 nm).
251 Absorption of red band is related to photosynthetic activity and reflectance of near-
252 infrared band is related to presence of vegetation canopies (Flynn, 2006). In drought
253 periods, NDVI values can reduce significantly, therefore many researchers have used this
254 index to measure drought events in recent years (Dalezios et al., 2014). To calculate NDVI
255 we will use this mathematical formula:

$$257 \quad NDVI = \frac{IR-R}{IR+R} \quad (2)$$

258
259 where IR and R are reflectance values in Near-Infrared band and Red band, respectively.
260 NDVI values below zero indicate no photosynthetic activity and are characteristic of areas
261 with large accumulation of water, such as rivers, lakes, or reservoirs. The higher is the
262 NDVI value, the greater is the photosynthetic activity and vegetation canopies.

263
264 In this paper, the NDVI is used, which is widely known index with a multitude of
265 applications over time. The NDVI is suited for monitoring of total vegetation, since it partly
266 compensates the changes in light conditions, land slope and field of view (Kundu et al.,
267 2016). In addition, clouds, water and snow show higher reflectance in the visible than in
268 the near infrared, thus, they have negative NDVI values. Indeed, bare and rocky terrain
269 show vegetation index values close to zero. Moreover, the NDVI constitutes a measure of
270 the degree of absorption by chlorophyll in the red band of the electromagnetic spectrum.
271 In summary, the NDVI is a reliable index of the chlorophyll density on the leaves, as well as
272 the percentage of the leaf area density over land, thus, NDVI constitutes a credible
273 measure for the assessment of dry matter (biomass) in various species vegetation cover
274 (Dalezios, 2013). It is clear from the above that the NDVI is an index closely related to
275 growth and development of plants, which can effectively monitor surface vegetation from
276 space.

277
278 The continuous increase of the NDVI value during the growing season reflects the
279 vegetative and reproductive growth due to intense photosynthetic activity, as well as the
280 satisfactory correlation with the final biomass production at the end of a growing period.
281 On the other hand, gradual decrease of the NDVI values signifies stress due to lack of
282 water or extremely high temperatures for the plants, leading to a reduction of the
283 photosynthetic rate and ultimately a qualitative and quantitative degradation of plants.
284 NDVI values above zero indicate the existence of green vegetation (chlorophyll), or bare
285 soil (values around zero), whereas values below zero indicate the existence of water,
286 snow, ice and clouds.

287

288 **2.2 Database**

289 Scientific research satellite Terra (EOS AM-1) has been chosen to provide necessary
290 information to calculate NDVI in the study area. This satellite was launched into orbit by
291 NASA on December 18, 1999. MODIS sensor aboard this satellite collects information of
292 different reflectance bands. MODIS information is organized by "products". The product
293 used in this study was MOD09A1 (LP DAAC, 2014). MOD09A1 incorporates seven
294 frequency bands: Band 1 (620-670 nm), band 2 (841-876 nm), band 3 (459-479 nm), band
295 4 (545-565 nm), 5 band (1230-1250 nm), band 6 (1628-1652 nm) and band 7 (2105-2155
296 nm). The bands used to calculate NDVI are: band 1 for red frequency and band 2 for near-
297 infrared frequency. MOD09A1 provides georeferenced images with pixel resolution of
298 500m x 500m. This product has a mix of the best reflectance measures of each pixel in an
299 8-days period. The period of time selected on this study was from 2002 to 2017.

300

301 Daily data from a **principal station** of the meteorological network were utilized during
302 the period studied (2002 – 2017). Meteorological station is located in 40°41'46"N
303 3°45'54"W (elevation 1004 m a.s.l.), less than 2 km from the study area (AEMET, 2017).

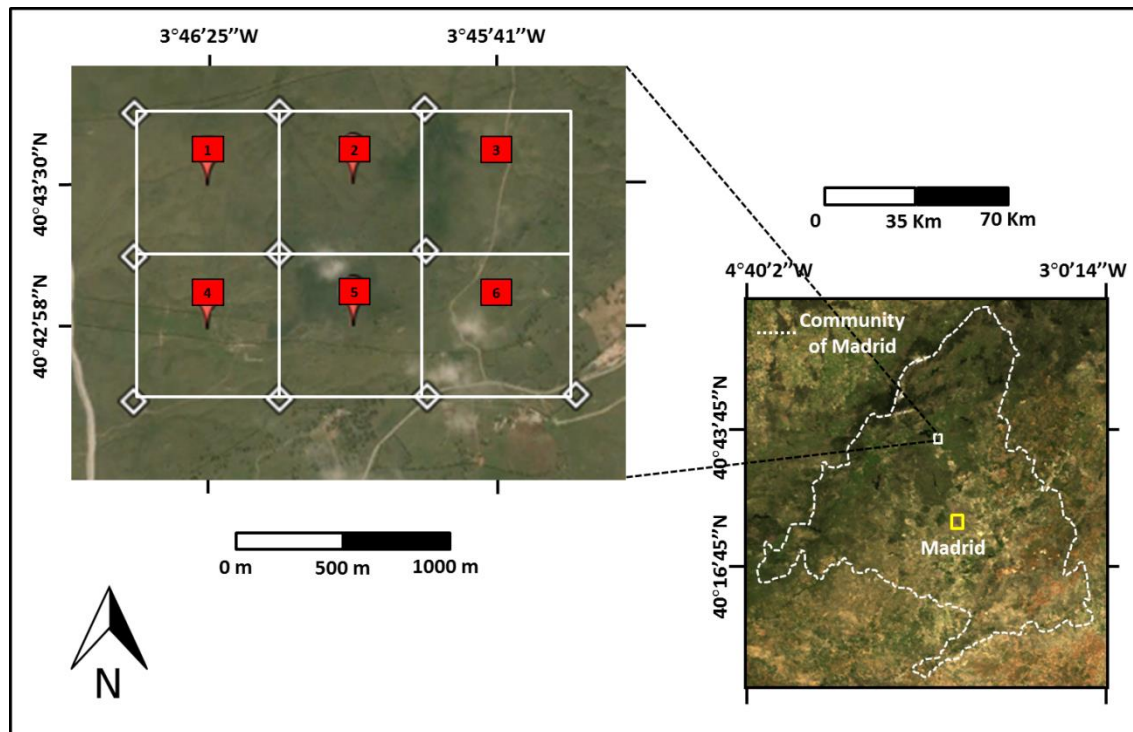
304

305 **2.3 Site description**

306 Six pixels (500m x 500m) are considered located in a pasture area at the north of the
307 Community of Madrid (Spain) between the municipalities of "Soto del Real" and
308 "Colmenar Viejo". The study area is located between meridians 3° 45' 00" and 3° 47' 00"
309 W and parallels 40° 42' 00" and 40° 44' 00" N approximately (see Fig. 1).

310

311



312

313 **Figure 1.** The study area is in the centre of the Iberian Peninsula (Community of Madrid). RGB
 314 image of six pixels area used for case study is shown (Google Earth's and MODIS images).

315

316 The annual mean temperature ranges during the study period from 12.7°C to 13.8°C,
 317 and annual mean precipitation ranges from 360 mm to 781 mm. The stations studied
 318 were identified semi-arid (annual ratio P/ETo between 0.2 and 0.5) according to the global
 319 aridity index developed by the United-Nations Convention to Combat Desertification
 320 (UNEP, 1997). According to the climatic classification of Köppen (Kottek et al., 2006), this
 321 area presents a continental Mediterranean climate temperate with dry and temperate
 322 summer (type Csb). Temperature and precipitation of this site, based on 20 years, is
 323 presented in Table 1.

324

325 Due to high soil moisture conditions, ash is the dominant tree, forming large
 326 agroforestry systems ("dehesas") that are used for pasture. These are ecosystems with
 327 high biodiversity.

328

329 **Table 1.** Monthly average of maximum temperature (Tmax), average temperature (Tavg),
 330 minimum temperature (Tmin) and precipitation (P). Study period from 1997 to 2017.

Month	Jan	Feb	Mar	Apr	May	Jun	Jul	Aug	Sep	Oct	Nov	Dec	Annual
Tmax (°C)	7.1	9.3	12.7	15.4	19.5	24.6	28.6	28.1	23.7	16.8	11.1	7.4	17.0
Tavg (°C)	3.6	4.8	7.7	10.1	13.7	18.4	22.0	21.7	17.9	12.3	7.1	4.1	12.0

Tmin (°C)	0.0	0.3	2.6	4.8	7.8	12.1	15.4	15.3	12.0	7.8	3.0	0.8	6.8
P (mm)	67.2	50.0	38.5	62.2	62.3	30.2	18.9	16.4	34.2	79.3	86.2	82.6	627.9

331

332 **2.4 HSL model**

333 There is no doubt that NDVI time-series from satellite sensors carry useful
 334 information, which can be used for characterizing seasonal dynamics of vegetation
 335 (Fensholt et al., 2012; Forkel et al., 2013). However, due to unfavorable atmospheric
 336 conditions during the data acquisition, NDVI time-series curve often contains noise
 337 (Motohka et al., 2011; Park, 2013). Although most of the NDVI data products are
 338 temporally composited through maximum value compositing (MVC) method (Holben,
 339 1986) to retain relatively cloud-free data, residual noise still exists in the data, which will
 340 affect the accuracy of the NDVI value.

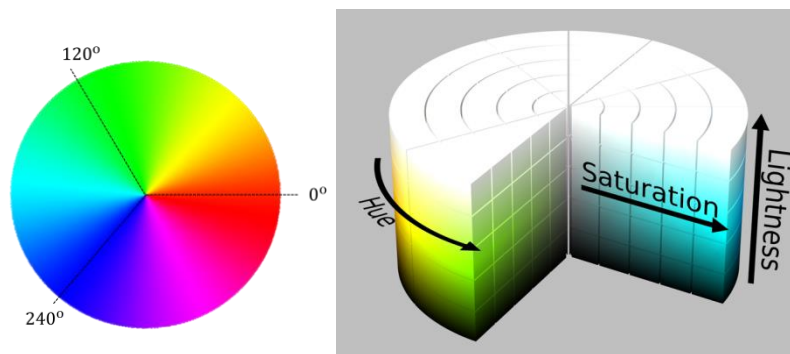
341

342 Therefore, usually it is necessary to reconstruct of NDVI time-series before extracting
 343 information from the noisy data. There are several techniques that have been applied to
 344 reduce noise and reconstruct NDVI series, a summary of these can be found in Wei et al.
 345 (2016). In this study we applied a simple filtering method based on the Hue-Saturation-
 346 Lightness (HSL) color model inspired by the work presented by Tackenberg (2007).

347

348 HSL color model is a cylindrical representation of RGB (Red-Green-Blue) points. Their
 349 components are Hue (color type), Saturation (level of color purity) and Lightness (color
 350 luminosity). Hue is the angular component and it is more intuitive for humans since it is
 351 directly related to the color wheel (see Fig. 2).

352



353

354 **Figure 2.** Colour wheel of Hue (on the left) and the HSL model (on the right).

355 Saturation is the radial component and near-zero values indicate grey colors.
 356 Lightness is the axial radial versus axial component, zero lightness produces black and full
 357 lightness produces white.

358

359 The NDVI series are filtered using the following HSL criterion: NDVI values are valid if
360 HSL Saturation is greater than 0.15. In this way, the values of the series that have grey
361 color correlate with pasture covered by clouds or snow are eliminated. This type of filter
362 based in HSL color space has been used on digital camera images monitoring vegetation
363 phenology (Tackenberg, 2007; Crimmins and Crimmins, 2008; Graham et al., 2009).
364 However, we have not found the use of this HSL criterion in the context of NDVI remote
365 sensing images.

366

367 **2.5 Maximum Likelihood Method (MLM)**

368 MLM estimates the set of parameters $\{\alpha, \beta, \mu, \sigma, \dots\}$ for a specific statistical
369 distribution that maximizes the “likelihood function” or the “joint density function”:

$$370 \quad L = f(\mathbf{x}, \boldsymbol{\theta}) = \prod_{i=1}^n f(x_i; \alpha, \beta, \mu, \sigma, \dots) \quad (3)$$

371 where $\mathbf{x} = (x_1, \dots, x_n)$ is the set of data, $\boldsymbol{\theta} = (\alpha, \beta, \mu, \sigma, \dots)$ is the vector of parameters
372 and $f(x_i; \alpha, \beta, \mu, \sigma, \dots)$ is the density function of the statistical model.

373 When maximization with respect to the vector of parameters is carried out, the
374 estimated parameters $(\hat{\alpha}, \hat{\beta}, \hat{\mu}, \hat{\sigma}, \dots)$ for the proposed statistical distribution are obtained
375 (Larson, 1982). Properties of estimated parameters are: invariance, consistency and
376 asymptotically unbiased.

377 In the case of a Gaussian model, the estimated statistics μ and σ are defined by
378 accurate expressions as follows:

$$379 \quad \hat{\mu} = \bar{x} = \frac{1}{n} \sum_{i=1}^n x_i \quad \hat{\sigma} = s = \sqrt{\frac{1}{n} \sum_{i=1}^n (x_i - \bar{x})^2} \quad (4)$$

380 where $\hat{\mu}$ is the sample mean and $\hat{\sigma}$ is the sample standard deviation of the data set.

381 In this study we will apply MLM to estimate the parameters for 4 probability density
382 functions (PDF). In Table 2, a brief description is presented of these PDF candidates:
383 Normal, Gamma, Beta and GEV. To do so, the following MATLAB functions have been
384 used: “normfit”, “gamfit”, “betafit” and “gevfit” (respectively).

385

386

Table 2. Candidate Probability Density Functions (PDF).

PDF NAME	PDF EXPRESSION	PDF PARAMETERS
----------	----------------	----------------

Normal	$f(x; \mu, \sigma) = \frac{1}{\sigma\sqrt{2\pi}} e^{-\frac{1}{2}\left(\frac{x-\mu}{\sigma}\right)^2}$	$\mu \equiv \text{average}$ $\sigma \equiv \text{standard deviation}$
Gamma	$f(x; \alpha, \beta) = \frac{1}{\beta^\alpha \Gamma(\alpha)} x^{\alpha-1} e^{-\frac{x}{\beta}}$	$\Gamma(\cdot) \equiv \text{gamma function}$ $\alpha \text{ and } \beta \equiv \text{parameters}$
Beta	$f(x; a, b) = \frac{\Gamma(a+b)}{\Gamma(a)\Gamma(b)} x^{a-1} (1-x)^{b-1}$	$\Gamma(\cdot) \equiv \text{gamma function}$ $a \text{ and } b \equiv \text{parameters}$
GEV	$f(x; \mu, \sigma, \xi) = \frac{1}{\sigma} t(x)^{\xi+1} e^{-t(x)}$ where $t(x) = \begin{cases} \left(1 + \left(\frac{x-\mu}{\sigma}\right)\xi\right)^{-1/\xi} & \text{if } \xi \neq 0 \\ e^{-(x-\mu)/\sigma} & \text{if } \xi = 0 \end{cases}$	$\mu \in \mathbb{R} \equiv \text{location param.}$ $\sigma > 0 \equiv \text{scale parameter}$ $\xi \in \mathbb{R} \equiv \text{shape parameter}$

387

388

389 **2.6 Goodness of fit (Chi-square test)**

390 χ^2 test can be used to determine to what extent observed frequencies differ from
391 frequencies expected for a specific statistical model. The most important points of the
392 theory are briefly presented in (Cochran, 1952).

393 Let $f(x, \theta)$ be a theoretical density function of a random variable X which depends on
394 parameters $\theta = (\alpha, \beta, \mu, \sigma, \dots)$ and let x_1, \dots, x_n be a sample of X grouped into k classes with n_i
395 data per class i .

396 Firstly, the following hypothesis is set:

397 (H_0) observed data fit theoretical distribution $f(x, \theta)$.

398 Then the test statistic χ_c^2 is defined as:

$$399 \quad \chi_c^2 = \sum_{i=0}^k \frac{(n_i - e_i)^2}{e_i} \quad (5)$$

400 where n_i is the number of data or observed frequency and $e_i = n \cdot P(\text{class } i)$ is the
401 expected frequency for class i . $P(\text{class } i)$ is the theoretical interval probability defined for
402 class i .

403 A level of significance is also set as:

$$404 \quad \alpha = P(\text{Reject } H_0 / H_0 \text{ is true}) \quad (6)$$

405 Finally, the following decision rule is applied: "reject the theoretical distribution at
406 significance level α if:

$$407 \quad \chi_c^2 > \chi_{(k-m-1, 1-\alpha)}^2 \quad (7)$$

408 where $\chi^2_{(k-m-1, 1-\alpha)}$ is a χ^2 distribution with k-m-1 degrees of freedom (m is the number of
409 parameters, k is the number of classes).

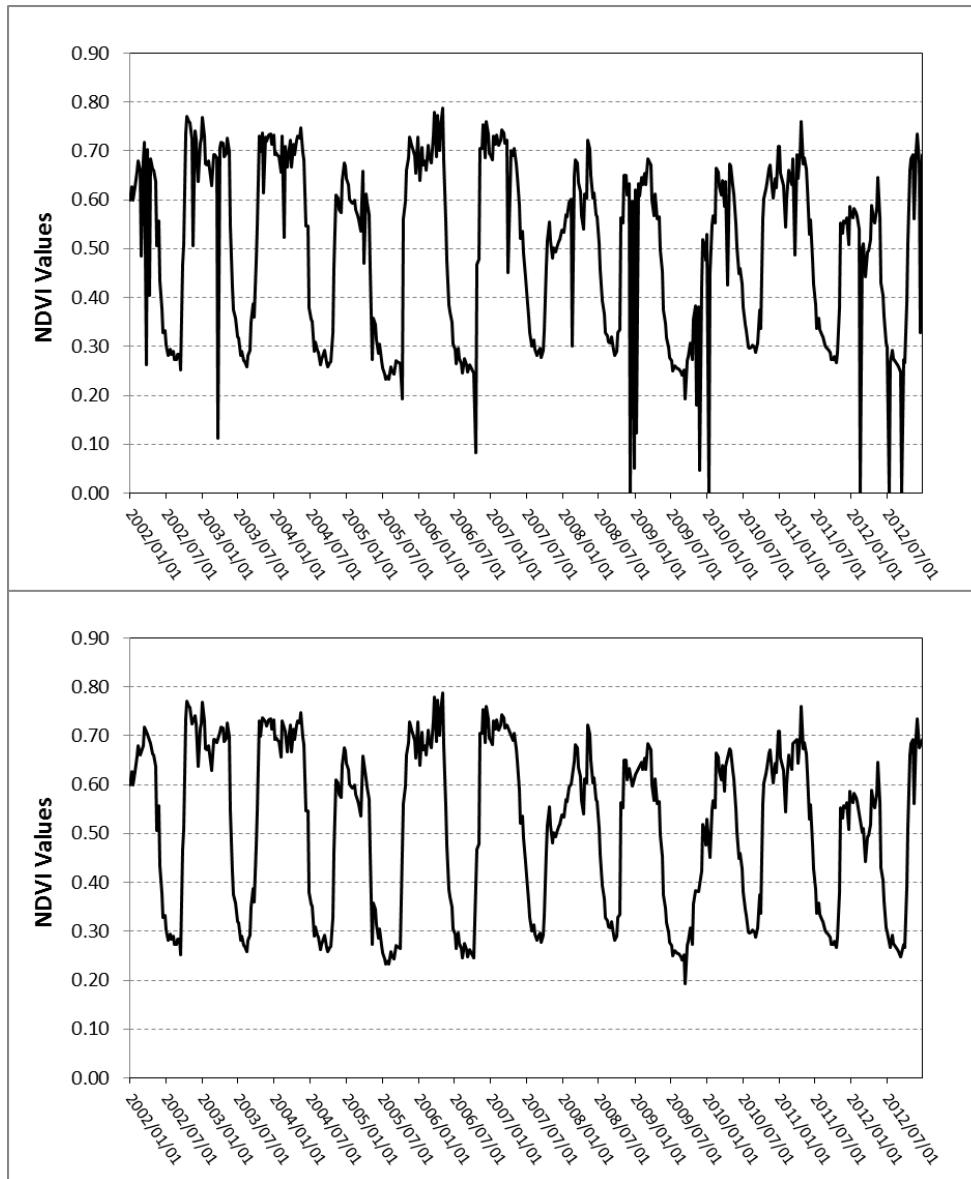
410

411

412 **3. Results and Discussion**

413 ***3.1 HSL filtering criterion***

414 NDVI series (from 2002 to 2017) were obtained for each pixel of the study area using
415 frequency bands provided by MODIS product named MOD09A1. These series contain
416 some irregular values that can skew NDVI pattern. Therefore, the six series (six pixels)
417 were filtered using the HSL criterion. **In Fig. 3 is shown an example of how HSL filtering
418 criterion works with a 10 years NDVI series (from 2002 to 2012).**



419

420 **Figure 3.** HSL filtering criterion applied to a 10 years NDVI series. Top graph shows the real NDVI
 421 series. Bottom graph shows the HSL filtered NDVI series.

422 The abrupt changes in the NDVI values, mainly observed during raining seasons such
 423 as autumn and winter, are efficiently eliminated. Not to be a high computational
 424 demanding method is one of the main advantages of HSL filtering method. Therefore, this
 425 method will allow us to obtain more robust NDVI values to be used in the statistical
 426 analysis.

427

428 **3.2 Maximum Likelihood Method (MLM) and Chi square test**

429 NDVI values were obtained consecutively every 8 days from MODIS product starting
 430 at 1st of January of every year, in such a way that 46 NDVI observations were considered
 431 for each year. Therefore, 46 Random Variables (RV) were defined when taking into
 432 account all the years of this study.

433 In Table 3, every RV (named as "Interval") can be seen together with the number of
 434 available NDVI observations. Each RV collects the observations coming from the six
 435 selected pixels. The start intervals of each season are: interval 45 for winter, interval 11
 436 for spring, interval 23 for summer and interval 34 for autumn.

437

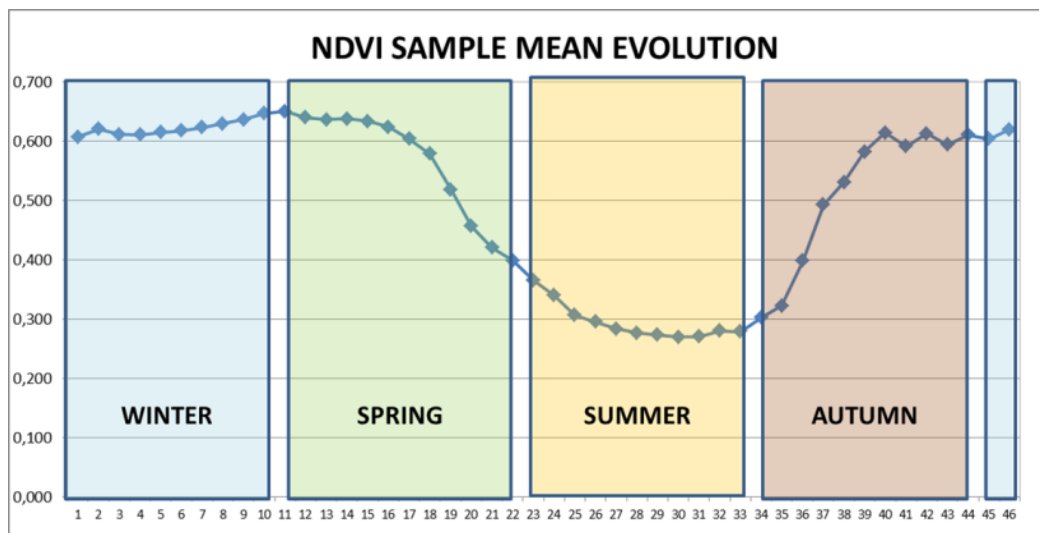
438 **Table 3.** Number of observations for every RV (named as Interval).

RANDOM VARIABLE	# OBSERVATIONS	RANDOM VARIABLE	# OBSERVATIONS
Interval 1	85	Interval 24	96
Interval 2	84	Interval 25	96
Interval 3	96	Interval 26	96
Interval 4	96	Interval 27	96
Interval 5	95	Interval 28	96
Interval 6	90	Interval 29	96
Interval 7	86	Interval 30	96
Interval 8	83	Interval 31	96
Interval 9	96	Interval 32	96
Interval 10	96	Interval 33	94
Interval 11	74	Interval 34	96
Interval 12	88	Interval 35	96
Interval 13	88	Interval 36	85
Interval 14	88	Interval 37	90
Interval 15	96	Interval 38	96
Interval 16	92	Interval 39	92
Interval 17	88	Interval 40	90
Interval 18	96	Interval 41	96
Interval 19	95	Interval 42	89
Interval 20	96	Interval 43	95
Interval 21	95	Interval 44	88
Interval 22	96	Interval 45	90
Interval 23	96	Interval 46	90

439

440

441 In Fig. 4, a plot with NDVI sample means of all RV with a start and end reference of the
442 astronomical seasons is shown. The typical evolution of the NDVI along a year can be
443 seen.
444



445
446 **Figure 4.** NDVI sample means of 46 random variables (RV) are shown as well as start and end
447 reference of every season. Study period from 2002 to 2017.

448
449 The observed evolution of NDVI through the different seasons is typical of the pasture
450 in this area. The summer presents the lowest mean values which begin to increase in
451 autumn achieving a maximum mean value of 0.60 or 0.65 during winter. In the middle of
452 the spring NDVI decrease again, approaching the lowest mean value of 0.28
453 approximately.

454
455 Taking into account these values, dense vegetation, in this study pasture, is found
456 from middle of October (interval 37) till the end of May (interval 19). It is in this period
457 where the precipitation concentrates (see Table 1). During the summer, the NDVI mean
458 values are lower than 0.3 corresponding with low precipitation and high temperatures.

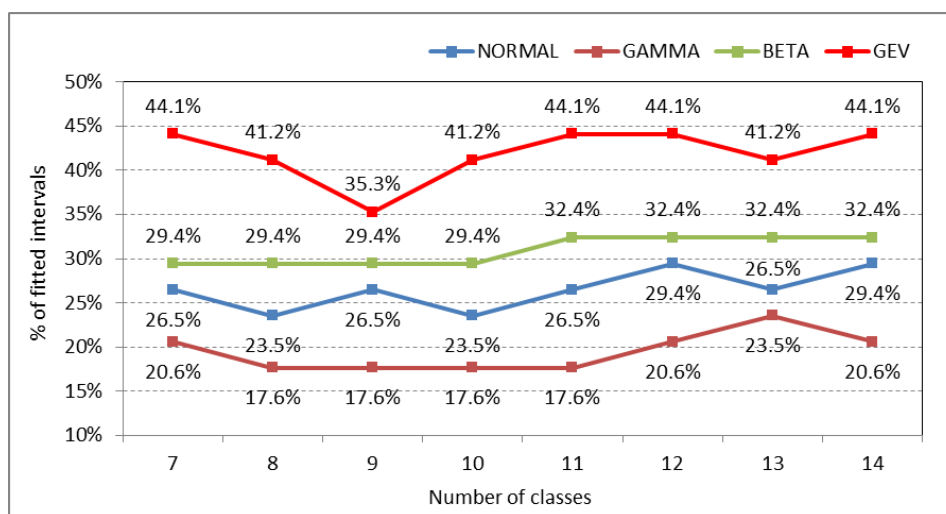
459
460 Following the work of Escribano-Rodriguez et al. (2014), there is a relationship of
461 pasture damage and a NDVI value around 0.40. Even if the authors point out that this
462 value is highly variable depending on the location, we can see that summer season in this
463 case study is under this value (see Fig. 4). This can explain that “Insurances for Damaged
464 Pasture” usually do not apply in these dates due to the arid environment (BOE, 2013).

465
466 MLM has been applied to model these 46 RV. Parameters have been calculated for 4
467 PDF (see Table 2) which are the candidates to be the best fit. To check the goodness of the

468 fit of PDF candidates, Chi square test (χ^2 test) has been used from 7 classes to 14 classes
 469 meeting the requirement that each class has at least five observations. The level of
 470 significance (α) was fixed to 5% for all the candidates.

471

472 Twelve intervals (from 23 to 34) corresponding to months of July, August and
 473 September have been excluded of this analysis since these intervals fall into the dry
 474 season in the study area, normally not cover by any SIBI. Therefore, calculations were
 475 carried out over 34 intervals. Fig. 5 shows the percentage of intervals that fit for every PDF
 476 candidate. The number of classes used in χ^2 test is represented at X-axis (from 7 to 14
 477 classes).



478

479 **Figure 5.** Percentage of fitted intervals (Y axis) for each PDF candidate (Normal, Gamma, Beta and
 480 GEV distributions) in function of the number of classes (X axis).

481

482 Fig. 5 indicates that GEV distributions explain more intervals (more than 40% for the
 483 majority of the class analysis) than Normal, Gamma or Beta distributions. An important
 484 difference between the Normal distribution and the rest of the PDF used in this work is its
 485 symmetry and kurtosis. Many of the observed NDVI distributions present a clear
 486 asymmetry and long tails in one or both sides that causes Normal distribution not to be
 487 the optimal fit.

488

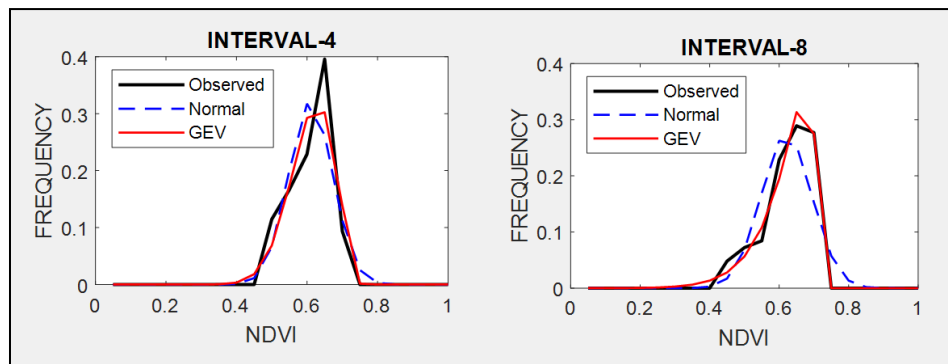
489 There is a relationship between seasons and the number of intervals that fit correctly.
 490 We found that GEV distributions explain better some intervals of spring and autumn since
 491 their observed distributions are very asymmetric. On the other hand, we did not find an
 492 important difference in winter, since its observed distributions are mainly symmetric.

493 Therefore, the methodology using the NDVI Normal assumption applied to design an
494 index-based insurance will not be feasible in many intervals of this study.

495

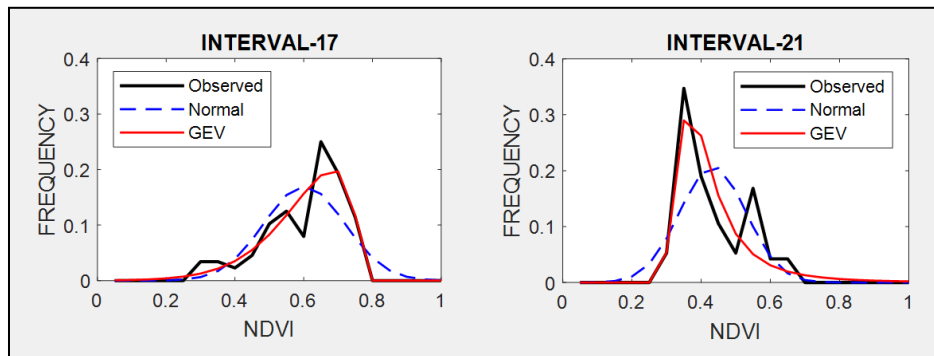
496 Table A1 at Appendix A shows the estimated parameters for each PDF and each
497 interval calculated by the MLM. These parameters were used to compare the estimated
498 PDF with the NDVI observed values on different times through the seasons. The following
499 intervals are shown as examples of better GEV fit: interval 4 and 8 (for winter, see Fig. 6),
500 interval 17 and 21 (for spring, see Fig. 7) and interval 36 and 40 (for autumn, see Fig. 8). In
501 these plots, observed frequency is compared versus Normal and GEV density distributions
502 calculated by MLM.

503



504

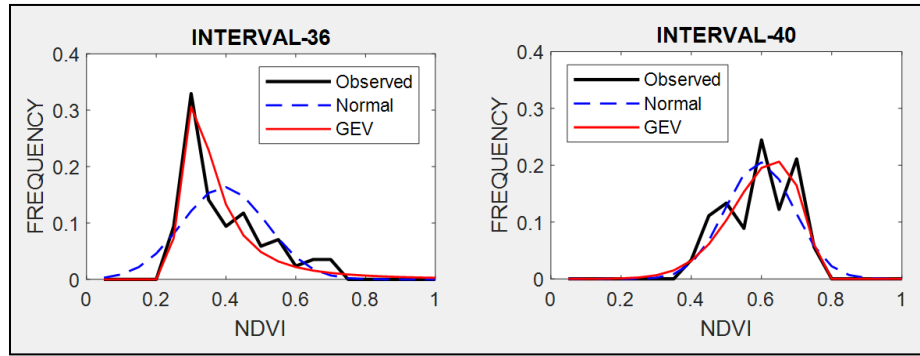
505 **Figure 6.** Comparison between observed NDVI frequency, GEV and Normal probability density
506 functions (PDF) on two different dates. Intervals 4 and 8 are examples for winter.



507

508 **Figure 7.** Comparison between observed NDVI frequency, GEV and Normal probability density
509 functions (PDF) on two different dates. Intervals 17 and 21 are examples for spring.

510



511

512 **Figure 8.** Comparison between observed NDVI frequency, GEV and Normal probability density
 513 functions (PDF) on two different times. Intervals 36 and 41 are examples for autumn.

514 During winter (see Fig. 6) the observed NDVI distribution presents negative skewness.
 515 Then, there is a higher frequency of high NDVI values corresponding with significant
 516 precipitation. During spring an evolution in the skewness is observed passing from
 517 negative to positive, and so, the lower NDVI values become the higher probable. Finally,
 518 during autumn precipitation begins and from positive pass to negative skewness and
 519 higher NDVI values are possible. We can observe that Normal distribution has no flexibility
 520 to follow this dynamic in the distributions on each time. This comparison is done in a
 521 sequential order for the whole of intervals in Figures A1, A2, A3 and A4 at Appendix A.

522

523 The more skewness and kurtosis depart from those of the Normal distribution the
 524 larger the errors affecting the insurance designed based on (Turvey et al., 2012). It is an
 525 expected result as pasture scenario is quite different from the development of a crop,
 526 where Normal distributions in the NDVI values are more expected. This high heterogeneity
 527 in time and space of NDVI estimated on pasture has been pointed out in several works
 528 (Martin-Sotoca et al, 2018). At the same time, more different is the observed NDVI
 529 frequency from a Normal distribution less representative is the average, and so, the
 530 median becomes a more representative value.

531

532 **3.3 Insurance context**

533 The use of NDVI thresholds in damaged pasture context was presented in the
 534 introduction section, being an example of using the "Insurance for Damaged Pasture" in
 535 Spain. We have chosen this last insurance to compare the results between applying
 536 Normal and GEV distribution methodologies. In this particular case the NDVI threshold
 537 ($NDVI_{th}$) was calculated using the expression $NDVI_{th} = \mu - k \cdot \sigma$ (where μ, σ are average and
 538 standard deviation of NDVI distributions respectively, assuming the Normal hypothesis).

539

540 The probability of being below $NDVI_{th}$ (using $k = 0.7$, first damage level in the
 541 insurance) at every interval has been calculated assuming the Normal hypothesis. As it
 542 was expected, this value is always 24.2% (see third column in Table 4). The probability of
 543 being below $NDVI_{th}$ has also been calculated using GEV distributions obtained in this
 544 study. The probability obtained by GEV distributions is mostly lower than the Normal
 545 distributions in spring, autumn and winter (see Table 4) that is the working period of the
 546 insurance.

547

548 Observing where in time are localized the highest relative error in probabilities (fifth
 549 column in Table 4), in absolute values, intervals corresponding to the end of winter,
 550 second middle of spring and the beginning of autumn present errors higher than 10%. This
 551 could explain why it is in spring and autumn when more disagreements exist between
 552 farmers and insurance company in claims.

553

554 **Table 4 – First column:** time intervals of approximately 8 days along the year. **Second column:** NDVI
 555 thresholds ($NDVI_{th}$) based on a Normal distribution applying $\mu - 0.7 \times \sigma$. **Third column:** percentages of
 556 area below the $NDVI_{th}$ when Normal distributions are applied. **Fourth column:** percentages of area
 557 below the $NDVI_{th}$ when GEV distributions are applied. **Fifth column:** relative area error of GEV
 558 compared to the Normal distribution.

559

RANDOM VARIABLE	NORMAL		GEV	
	$NDVI_{th}$	Prob.	Prob.	Error (%)
Interval 1	0.535	24.20%	24.37%	0.70%
Interval 2	0.541	24.20%	23.18%	-4.21%
Interval 3	0.541	24.20%	23.27%	-3.84%
Interval 4	0.543	24.20%	23.27%	-3.84%
Interval 5	0.545	24.20%	24.17%	-0.12%
Interval 6	0.534	24.20%	21.48%	-11.24%
Interval 7	0.528	24.20%	24.01%	-0.79%
Interval 8	0.546	24.20%	20.70%	-14.46%
Interval 9	0.555	24.20%	21.30%	-11.98%
Interval 10	0.561	24.20%	22.28%	-7.93%
Interval 11	0.567	24.20%	23.49%	-2.93%
Interval 12	0.572	24.20%	23.75%	-1.86%
Interval 13	0.571	24.20%	23.20%	-4.13%
Interval 14	0.570	24.20%	24.29%	0.37%
Interval 15	0.571	24.20%	23.47%	-3.02%

Interval 16	0.560	24.20%	23.26%	-3.88%
Interval 17	0.495	24.20%	21.29%	-12.02%
Interval 18	0.484	24.20%	21.58%	-10.83%
Interval 19	0.442	24.20%	23.06%	-4.71%
Interval 20	0.381	24.20%	27.20%	12.40%
Interval 21	0.342	24.20%	29.46%	21.74%
Interval 22	0.323	24.20%	28.84%	19.17%
Interval 35	0.257	24.20%	18.98%	-21.57%
Interval 36	0.285	24.20%	28.57%	18.06%
Interval 37	0.333	24.20%	25.90%	7.02%
Interval 38	0.398	24.20%	24.27%	0.29%
Interval 39	0.454	24.20%	23.79%	-1.69%
Interval 40	0.503	24.20%	22.81%	-5.74%
Interval 41	0.491	24.20%	23.23%	-4.01%
Interval 42	0.517	24.20%	24.66%	1.90%
Interval 43	0.507	24.20%	23.13%	-4.42%
Interval 44	0.514	24.20%	23.49%	-2.93%
Interval 45	0.515	24.20%	23.70%	-2.07%
Interval 46	0.509	24.20%	23.33%	-3.60%

560

561 In Table 4, Normal $NDVI_{th}$ have been used to calculate the probability in GEV distributions.
562 An alternative calculation can be the use of Normal probability (24.2%) to calculate new
563 $NDVI_{th}$ based on GEV (see Table 5). It can be seen that new $NDVI_{th}$ obtained by GEV
564 distributions are mostly upper than thresholds using Normal distributions in spring,
565 autumn and winter. Considering these results we find that damage thresholds calculated
566 by GEV methodology are mostly above that one's calculated by Normal methodology.

567 Again, intervals corresponding to the end of winter, second middle of spring and the
568 beginning of autumn present $NDVI_{th}$ relative errors higher than 1% in absolute values
569 (fourth column in Table 5).

570

571 **Table 5 - First column:** time intervals of approximately 8 days along the year. **Second column:** NDVI
572 thresholds ($NDVI_{Th}$) based on a Normal distribution (Normal) applying $\mu - 0.7 \times \sigma$. **Third column:**
573 $NDVI_{Th}$ based on a GEV distribution (GEV) using 24.2% as the area below the $NDVI_{Th}$. **Fourth column:**
574 relative $NDVI_{Th}$ error of GEV compared to the Normal distribution.

575

RANDOM VARIABLE	NDVI _{Th}		Error (%)
	Normal	GEV	
Interval 1	0.535	0.534	-0,19%
Interval 2	0.541	0.543	0,37%
Interval 3	0.541	0.543	0,37%
Interval 4	0.543	0.545	0,37%
Interval 5	0.545	0.545	0,00%
Interval 6	0.534	0.543	1,69%
Interval 7	0.528	0.528	0,00%
Interval 8	0.546	0.558	2,20%
Interval 9	0.555	0.563	1,44%
Interval 10	0.561	0.567	1,07%
Interval 11	0.567	0.569	0,35%
Interval 12	0.572	0.574	0,35%
Interval 13	0.571	0.574	0,53%
Interval 14	0.570	0.569	-0,18%
Interval 15	0.571	0.573	0,35%
Interval 16	0.560	0.563	0,54%
Interval 17	0.495	0.510	3,03%
Interval 18	0.484	0.498	2,89%
Interval 19	0.442	0.447	1,13%
Interval 20	0.381	0.374	-1,84%
Interval 21	0.342	0.334	-2,34%
Interval 22	0.323	0.318	-1,55%
Interval 35	0.257	0.262	1,95%
Interval 36	0.285	0.278	-2,46%
Interval 37	0.333	0.327	-1,80%
Interval 38	0.398	0.398	0,00%
Interval 39	0.454	0.455	0,22%
Interval 40	0.503	0.508	0,99%
Interval 41	0.491	0.494	0,61%
Interval 42	0.517	0.516	-0,19%
Interval 43	0.507	0.510	0,59%
Interval 44	0.514	0.516	0,39%
Interval 45	0.515	0.516	0,19%
Interval 46	0.509	0.511	0,39%

576

577

578 **4. Conclusions**

579 According to the results obtained in the study area using MLM and χ^2 test, it can be
580 concluded that Normal distributions are not the best fit to the NDVI observations, and
581 GEV distributions provide a better approximation.

582

583 The difference between Normal and GEV assumption is more evident in the transition
584 from winter to summer (spring), where NDVI values decrease, and then from summer to
585 winter (autumn) presenting the opposite behavior of increasing NDVI values. In both
586 periods asymmetrical distributions were found, negative skewness for the spring
587 transition and positive skewness for the autumn transition. During both periods the
588 variability in precipitation and temperatures were higher in this location.

589

590 We have found differences if GEV assumption is selected instead of the Normal one
591 when defining damaged pasture thresholds ($NDVI_{th}$). The use of these different
592 assumptions should be taken into account in future insurance implementations due to the
593 important consequences of supposing a damage event or not. We propose the use of
594 **quantiles** in observed NDVI distributions instead of average and standard deviation,
595 typically of Normal distributions, to calculate new $NDVI_{th}$.

596

597

598

599

600 **Acknowledgements**

601 This research has been partially supported by funding from MINECO under contract No.
602 MTM2015-63914-P and CICYT PCIN-2014-080.

603

604 **Appendix A**

605

606

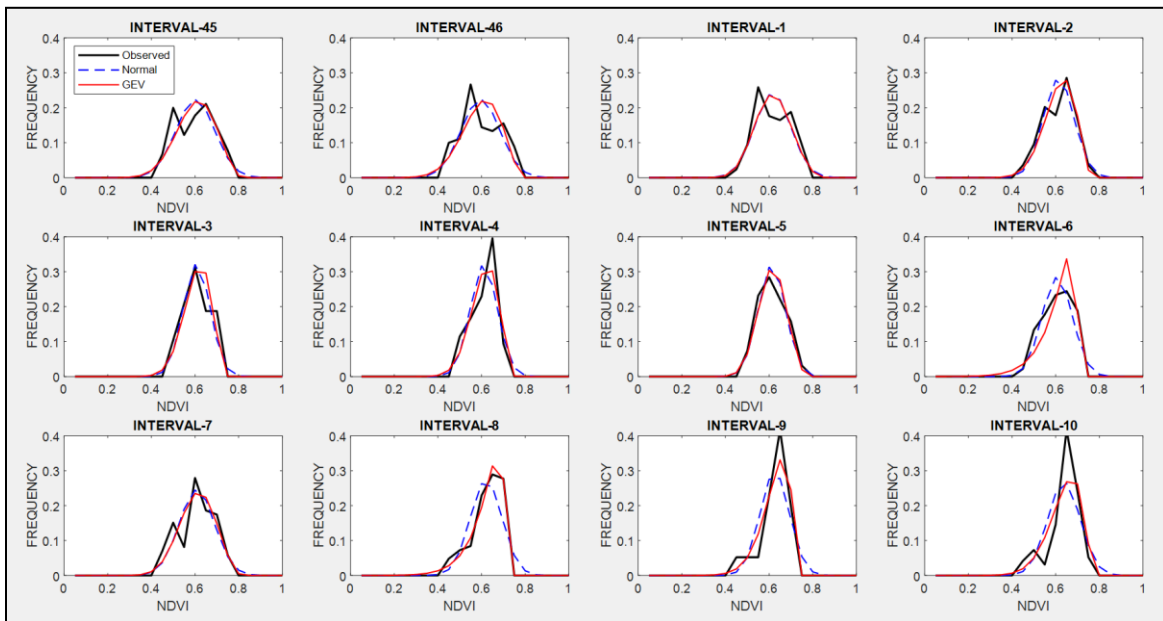
Table A1 - Maximum Likelihood parameters calculated for 4 PDF.

RANDOM VARIABLE	NORMAL		GAMMA		BETA		GEV		
	μ	σ	α	β	a	b	μ	σ	ξ
Interval 1	0.591	0.081	53.31	0.011	21.45	14.82	0.563	0.080	-0.297
Interval 2	0.589	0.069	71.14	0.008	30.62	21.40	0.571	0.073	-0.477
Interval 3	0.583	0.060	94.15	0.006	39.56	28.34	0.567	0.063	-0.457
Interval 4	0.585	0.060	91.88	0.006	39.58	28.05	0.570	0.064	-0.468
Interval 5	0.588	0.061	93.92	0.006	38.83	27.25	0.568	0.061	-0.340
Interval 6	0.582	0.068	70.28	0.008	30.67	22.05	0.577	0.083	-0.846
Interval 7	0.584	0.080	52.52	0.011	22.16	15.82	0.559	0.082	-0.366
Interval 8	0.596	0.071	65.37	0.009	28.89	19.59	0.591	0.081	-0.833
Interval 9	0.601	0.066	76.02	0.008	34.31	22.84	0.590	0.070	-0.652
Interval 10	0.613	0.073	63.83	0.010	27.80	17.62	0.598	0.079	-0.572
Interval 11	0.621	0.078	58.72	0.011	24.33	14.86	0.600	0.083	-0.451
Interval 12	0.624	0.073	68.33	0.009	28.01	16.94	0.603	0.078	-0.431
Interval 13	0.624	0.075	66.22	0.009	26.23	15.85	0.604	0.080	-0.476
Interval 14	0.631	0.088	50.23	0.013	18.71	10.92	0.603	0.090	-0.342
Interval 15	0.630	0.084	53.60	0.012	21.17	12.45	0.607	0.089	-0.448
Interval 16	0.627	0.096	38.75	0.016	16.08	9.59	0.602	0.103	-0.474
Interval 17	0.577	0.117	20.47	0.028	10.24	7.58	0.560	0.127	-0.692
Interval 18	0.568	0.120	20.52	0.028	9.71	7.42	0.552	0.136	-0.718
Interval 19	0.523	0.116	19.46	0.027	9.52	8.68	0.495	0.125	-0.493
Interval 20	0.452	0.101	20.99	0.022	10.98	13.31	0.401	0.077	0.078
Interval 21	0.409	0.095	19.94	0.021	11.18	16.13	0.354	0.060	0.325
Interval 22	0.379	0.080	24.66	0.015	14.41	23.52	0.333	0.046	0.385
Interval 23	0.353	0.073	26.54	0.013	15.85	29.01	0.311	0.036	0.456
Interval 24	0.328	0.056	38.36	0.009	24.22	49.65	0.298	0.033	0.287
Interval 25	0.305	0.044	53.52	0.006	35.62	81.20	0.282	0.028	0.210
Interval 26	0.298	0.034	78.93	0.004	54.47	128.55	0.283	0.029	-0.064
Interval 27	0.289	0.026	126.85	0.002	88.33	217.15	0.278	0.021	-0.030
Interval 28	0.282	0.022	166.17	0.002	119.50	305.03	0.274	0.022	-0.322
Interval 29	0.278	0.021	179.09	0.002	127.93	332.63	0.269	0.018	-0.085
Interval 30	0.273	0.019	203.11	0.001	147.67	393.21	0.266	0.019	-0.247
Interval 31	0.272	0.022	166.83	0.002	120.11	321.95	0.262	0.018	-0.059
Interval 32	0.280	0.034	75.63	0.004	52.36	134.30	0.264	0.023	0.118
Interval 33	0.285	0.034	82.05	0.004	54.90	137.68	0.270	0.020	0.122
Interval 34	0.295	0.057	33.26	0.009	21.15	50.37	0.268	0.024	0.363

Interval 35	0.312	0.079	19.70	0.016	11.83	25.94	0.275	0.038	0.300
Interval 36	0.369	0.121	10.81	0.034	6.11	10.33	0.298	0.063	0.480
Interval 37	0.432	0.141	9.45	0.046	5.21	6.81	0.370	0.120	-0.080
Interval 38	0.487	0.128	13.88	0.035	7.25	7.63	0.445	0.127	-0.321
Interval 39	0.529	0.107	23.56	0.022	11.39	10.16	0.497	0.110	-0.390
Interval 40	0.570	0.096	34.02	0.017	15.10	11.40	0.548	0.105	-0.533
Interval 41	0.554	0.090	36.42	0.015	16.90	13.64	0.531	0.096	-0.471
Interval 42	0.583	0.095	37.29	0.016	15.56	11.11	0.551	0.094	-0.295
Interval 43	0.574	0.097	34.27	0.017	14.93	11.07	0.550	0.103	-0.482
Interval 44	0.572	0.083	47.13	0.012	20.40	15.26	0.549	0.086	-0.425
Interval 45	0.576	0.088	42.59	0.014	18.17	13.36	0.550	0.090	-0.396
Interval 46	0.570	0.088	41.98	0.014	18.11	13.66	0.546	0.092	-0.445

607

608



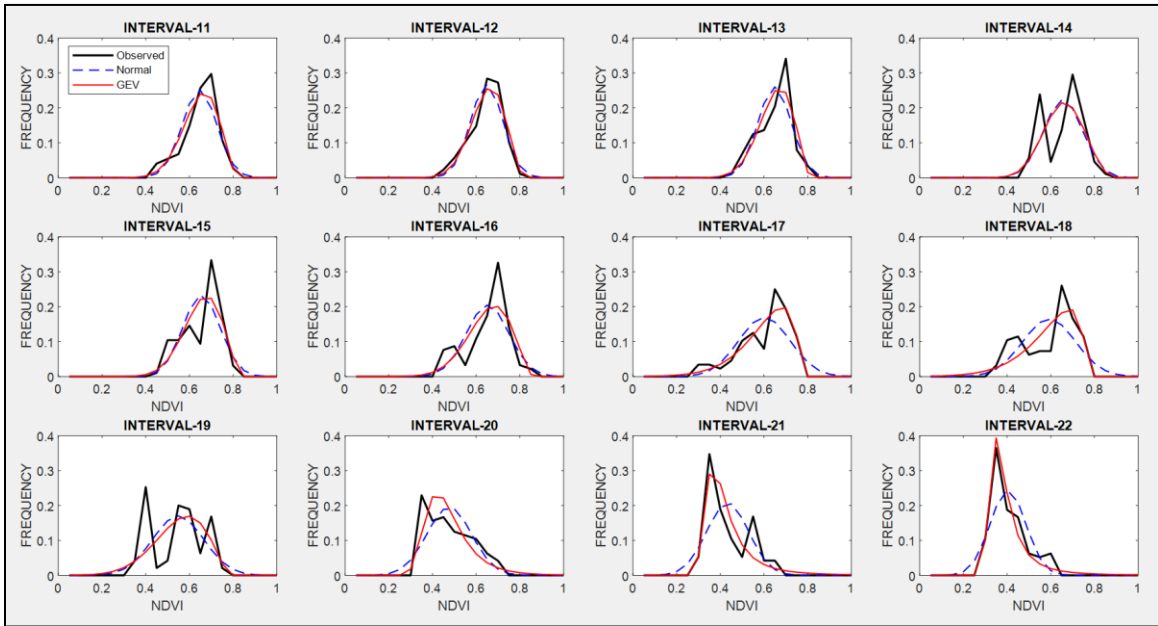
609

610

611

Figure A1. Observed NDVI, GEV and Normal probability density functions (PDF) from interval 45 to interval 10 (from 19 December to 21 March) representing winter.

612



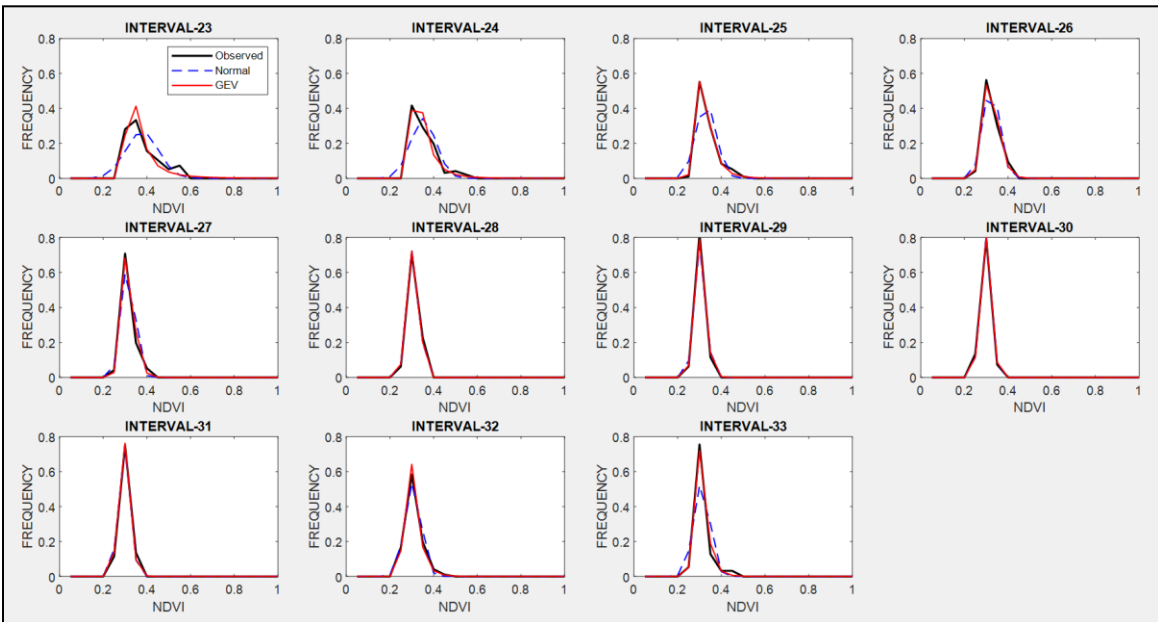
613

614

615

Figure A2. Observed NDVI, GEV and Normal probability density functions (PDF) from interval 11 to interval 22 (from 22 March to 25 June) representing spring.

616



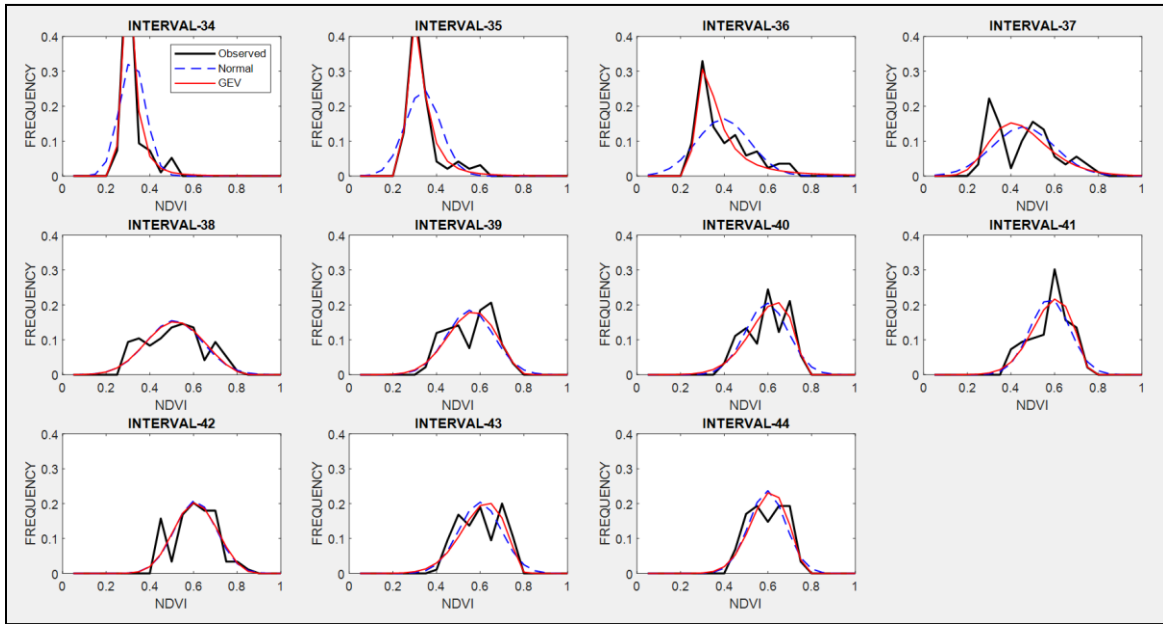
617

618

619

Figure A3. Observed NDVI, GEV and Normal probability density functions (PDFs) from interval 23 to interval 33 (from 26 June to 21 September) representing summer.

620



621

622

623

Figure A4. Observed NDVI, GEV and Normal PDFs from interval 34 to interval 44 (from 22 September to 18 December) representing autumn.

624

625 **References**

626

627 Agencia Estatal de Meteorología (AEMET). Available at: www.aemet.es, 2017.

628 Al-Bakri, J. T., and Taylor, J. C.: Application of NOAA AVHRR for monitoring vegetation
629 conditions and biomass in Jordan, *J. Arid Environ*, 54, 579–593, 2003.

630 Bailey, S.: The Impact of Cash Transfers on Food Consumption in Humanitarian Settings: A
631 review of evidence, Study for the Canadian Foodgrains Bank, May 2013.

632 Boletín Oficial del Estado (BOE, 6638 - Orden AAA/1129/2013. Nº 145, III, p-46077, 2013.

633 Cochran, William G.: The Chi-square Test of Goodness of Fit, *Annals of Mathematical
634 Statistics*. 23: 315–345, 1952.

635 Crimmins, M. A., and Crimmins T. M.: Monitoring plant phenology using digital repeat
636 photography, *Environ. Manage*, 41, 949-958, 2008.

637 Dalezios, N. R., Blanta, A., Spyropoulos, N. V., and Tarquis A. M.: Risk identification of
638 agricultural drought for sustainable Agroecosystems, *Nat. Hazards Earth Syst. Sci.*, 14,
639 2435–2448, 2014.

640 Dalezios, N. R.: The Role of Remotely Sensed Vegetation Indices in Contemporary
641 Agrometeorology. Invited paper in Honorary Special Volume in memory of late Prof. A.
642 Flokas. Publisher: Hellenic Meteorological Association, 33-44, 2013.

643 De Leeuw, J., Vrieling, A., Shee, A., Atzberger, C., Hadgu, K. M., Biradar, C. M., Humphrey
644 Keah, H., and Turvey, C.: The Potential and Uptake of Remote Sensing in Insurance: A
645 Review, *Remote Sens.*, 6(11), 10888-10912, 2014.

646 Escribano Rodríguez, J. Agustín, Díaz-Ambrona, Carlos Gregorio H., and Tarquis Alfonso,
647 Ana María: Selection of vegetation indices to estimate pasture production in Dehesas,
648 *PASTOS*, 44(2), 6-18, 2014.

649 Fensholt, R., and Proud, S. R.: Evaluation of earth observation based global long term
650 vegetation trends - comparing GIMMS and MODIS global NDVI time series, *Remote
651 Sens. Environ.*, 119, 131–147, 2012.

652 Flynn E. S.: Using NDVI as a pasture management tool. Master Thesis, University of
653 Kentucky, 2006.

654 Forkel, M., Carvalhais, N., Verbesselt, J., Mahecha, M.D., Neigh, C. S., and Reichstein, M.:
655 Trend change detection in NDVI time series: effects of inter-annual variability and
656 methodology, *Remote Sens.*, 5, pp, 2113–2144, 2013.

657 Fuller, D.O.: Trends in NDVI time series and their relation to rangeland and crop production
658 in Senegal, 1987–1993, *Int. J. Remote Sens.*, 19, 2013–2018, 1998.

659 Gommers, R., and Kayitakire, F.: The challenges of index-based insurance for food security
660 in developing countries. Proceedings, Technical Workshop, JRC, Ispra, 2-3 May 2012.
661 Publisher: JRC-EC, p. 276, 2013.

662 Gouveia, C., Trigo, R. M., and Da Camara, C. C.: Drought and vegetation stress monitoring
663 in Portugal using satellite data, *Nat. Hazards Earth Syst. Sci.*, 9, 185-195, 2009.

664 Goward, S. N., Tucker, C. J., and Dye, D.G.: North-American vegetation patterns observed
665 with the NOAA-7 advanced very high-resolution radiometer. *Vegetation*, 64, 3–14,
666 1985.

667 Graham, E. A., Yuen, E. M., Robertson, G. F., Kaiser, W. J., Hamilton, M. P., and Rundel, P.
668 W.: Budburst and leaf area expansion measured with a novel mobile camera system
669 and simple color thresholding, *Environ. Exp. Bot.*, 65, 238-244, 2009.

670 Hobbs, T. J.: The use of NOAA-AVHRR NDVI data to assess herbage production in the arid
671 rangelands of central Australia, *Int. J. Remote Sens.*, 16, 1289–1302, 1995.

672 Holben, B. N.: Characteristics of maximum-value composite images from temporal AVHRR
673 data, *Int. J. Remote Sens.*, 7, 1417–1434, 1986.

674 Kottek, M., Grieser, J., Beck, C., Rudolf, B., and Rubel, F.: World Map of the Köppen-Geiger
675 climate classification updated, *Meteorologische Zeitschrift*, 15, 259-263, 2006.

676 Kundu, A., Dwivedi, S., and Dutta, D.: Monitoring the vegetation health over India during
677 contrasting monsoon years using satellite remote sensing indices, *Arab J Geosci.*, 9,
678 144, 2016.

679 Land Processes Distributed Active Archive Center (LP DAAC): Surface Reflectance 8-Day L3
680 Global 500m. NASA and USGS. Available at:
681 https://lpdaac.usgs.gov/products/modis_products_Table/mod09a1. 2014.

682 Larson, H. J.: *Introduction to Probability Theory and Statistical Inference* (3rd edition). New
683 York, John Wiley and Sons, 1982.

684 Leblois, A.: Weather index-based insurance in a cash crop regulated sector: ex ante
685 evaluation for cotton producers in Cameroon. Paper presented at the JRC/IRI
686 workshop on The Challenges of Index-Based Insurance for Food Security in Developing
687 Countries, Ispra, 2-3, May, 2012.

688 Lovejoy, S., Tarquis, A. M., Gaonac’h, H., and Schertzer, D.: Single and Multiscale remote
689 sensing techniques, multifractals and MODIS derived vegetation and soil moisture.
690 *Vadose Zone J.*, 7, 533-546, 2008.

691 Maples, J. G., Brorsen, B. W., and Biermachs, J. T.: The rainfall Index Annual Forage pilot
692 program as a risk management tool for cool-season forage. *J. Agr. Appl Econ*, 48(1),
693 29–51, 2016.

694 Martin-Sotoca, J. J., Saa-Requejo, A., Orondo J. B., and Tarquis, A. M.: Singularity maps
695 applied to a vegetation index. *Bio. Eng.* 168, 42-53, 2018.

696 Motohka, T., Nasahara, K. N., Murakami, K., and Nagai, S.: Evaluation of sub-pixel cloud
697 noises on MODIS daily spectral indices based on in situ measurements, *Remote Sens.*,
698 3, 1644–1662, 2011.

699 Niemeyer, S.: New drought indices, First Int. Conf. on Drought Management: Scientific and
700 Technological Innovations, Zaragoza, Spain. Joint Research Centre of the European
701 Commission, Available online at
702 <http://www.iamz.ciheam.org/medroplan/zaragoza2008/Sequia2008/Session3/S.Niemeyer.pdf>, 2008.
703

704 Ortega-Farias, S., Ortega-Salazar, S., Poblete, T., Kilic, A., Allen, R., Poblete-Echeverría, C.,
705 Ahumada-Orellana, L., Zuñiga, M., and Sepúlveda, D.: Estimation of Energy Balance
706 Components over a Drip-Irrigated Olive Orchard Using Thermal and Multispectral
707 Cameras Placed on a Helicopter-Based Unmanned Aerial Vehicle (UAV), *Remote Sens.*,
708 8, 638, pp 18, 2016.

709 Park, S.: Cloud and cloud shadow effects on the MODIS vegetation index composites of the
710 Korean Peninsula, *Int. J. Remote Sens.*, 34, 1234–1247, 2013.

711 Rao, K. N.: Index based Crop Insurance, *Agric. Agric. Sci. Proc.*, 1, 193–203, 2010.

712 Roumiguié, A., Sigel, G., Poilvé, H., Bouchard, B., Vrieling, A., and Jacquin, A.: Insuring
713 forage through satellites: testing alternative indices against grassland production
714 estimates for France, *Int. J. Remote Sens.*, 38, 1912-1939, 2017.

715 Roumiguié, A., Jacquin, A., Sigel, G., Poilvé, H., Lepoivre, B., and Hagolle, O.: Development
716 of an index-based insurance product: validation of a forage production index derived
717 from medium spatial resolution fCover time series, *GIScience Remote Sens.*, 52, 94-
718 113, 2015.

719 Tackenberg, Oliver: A New Method for Non-destructive Measurement of Biomass, Growth
720 Rates, Vertical Biomass Distribution and Dry Matter Content Based on Digital Image
721 Analysis, *Annals of Botany*, 99(4), 777–783, 2007.

722 Turvey, C. G., and Mcaurin, M. K.: Applicability of the Normalized Difference Vegetation
723 Index (NDVI) in Index-Based Crop Insurance Design, *Am. Meteorol. Soc.*, 4, 271-284,
724 2012.

725 UNEP Word Atlas of Desertification: Second Ed. United Nations Environment Programme,
726 Nairobi, 1997.

727 USDA. U.S. Department of Agriculture, Federal Crop Insurance Corporation, Risk
728 Management Agency: Rainfall Index Plan Annual Forage Crop Provisions. 16- RI-AF.
729 <http://www.rma.usda.gov/policies/ri-vi/2015/16riaf.pdf> 2013 (Accessed March 1,
730 2018).

731 Wei, W., Wu, W., Li, Z., Yang, P., and Qingbo Zhou, Q.: Selecting the Optimal NDVI Time-
732 Series Reconstruction Technique for Crop Phenology Detection, *Intell. Autom. Soft. Co.*
733 22, 237-247, 2016.
734
735
736
737